RSMC Tokyo – Typhoon Center

# *Technical Review*

No. 7

Contents



Japan Meteorological Agency

March 2004

# Improvement of the JMA Typhoon Model by Using New Physical Processes

**Ryota Sakai, Takuya Hosomi**

*Numerical Prediction Division, Japan Meteorological Agency*

**Abstract**

The Typhoon Model (TYM) with a new physical process package was operationally implemented in July 2003 at the Japan Meteorological Agency (JMA). In this package, (1) a prognostic cloud scheme based on Smith (1990) and (2) a radiation scheme including the direct effect of aerosols were newly introduced. In addition to these effect, (3) a prognostic Arakawa-Schubert cumulus parameterization scheme and (4) estimation of the roughness length on the sea surface were modified. The schemes (1) to (3) had already been implemented into the Global Spectral Model (GSM) by Kuma et al. (2001). Preliminary experiments with three typhoons in 2002 were carried out for 108 cases. The results showed remarkable improvements in track prediction and neutral skill in intensity prediction of typhoon.

## 1. Introduction

JMA operates TYM four times a day for the prediction of tropical cyclones in the western North Pacific. In recent years, TYM has been improved by changing the typhoon bogus system (e.g., Sakai et al. 2002), while the GSM has been improved by changing the physical processes and succeeds to reduce the typhoon positional error (e.g., Kuma et al. 2001). Based on the above improvement in GSM, the physical processes of TYM are changed by introducing a physical process package, which was implemented in GSM in December 1999 (GSM9912).

In this paper, the new physical process package for TYM and its performance are presented. First, the modifications on physical processes from the previous TYM are introduced in section 2. The result of the experiment is shown in section 3. Finally, a summary of the result and concluding remarks are presented in section 4.

## 2. Improvements on the physical processes

The improvements on the physical processes of TYM consist of two components:

(1) Introduction of the physical process package of GSM9912

The new physical process package includes

(a) Introduction of a prognostic cloud water scheme (Smith 1990),

(b) Introduction of the direct effect of aerosols on short-wave radiation,

(c) Modification of the prognostic Arakawa-Schubert cumulus parameterization scheme.

Hosomi (2002) reported that by introducing the physical process package of GSM9912 into the Regional Spectral Model (RSM), the skill of the upper-tropospheric wind became better and meso-scale lows spuriously generated by intensive false rain were suppressed. Since TYM has the same dynamical frame and physical processes as RSM, the new TYM is expected to improve the track prediction of typhoon in the same way as RSM.

(2) Modification of the roughness length on the sea surface

Preliminary experiments showed, however, that TYM with the new physical processes mentioned above often overestimated typhoon intensity. It is known that simulated typhoon intensity is sensitive not only to the cumulus parameterization but also to the parameterization of heat (and water vapor) and momentum fluxes from the sea surface. Some recent studies indicate that the intensity of a simulated tropical cyclone is sensitive to the ratio of the exchange coefficients Ch/Cm, where Ch the exchange coefficient of heat (and water vapor) and Cm the exchange coefficient of momentum. The lower the value of Ch/Cm, the weaker a intensity of the simulated tropical cyclone (Emanuel 1995; Bao 2002 ). In order to suppress the overestimation in typhoon intensity forecasts, the parameterization of roughness length on the sea surface is changed so that the heat and moisture fluxes on the sea surface are decreased (Lower value of Ch/Cm). For this purpose,

(d) The roughness length formulae in TYM are changed from Kondo (1975) to Garratt (1992) and Beljaars (1995). Garratt (1992) is used for the heat (and water vapor) exchange coefficient, Beljaars (1995) is used for the momentum exchange coefficient.

Details of the change to the roughness length on the sea surface are described in APPENDIX.

## 3. Results

In order to examine the forecast performance for various typhoons, the following three typhoons are selected by considering the seasonal condition and the typhoon track (Fig. 1):

- T0206 (CHATAAN): 29 June to 11 July 2002 with recurvature.
- T0216 (SINLAKU): 29 August to 7 September 2002 without recurvature.
- T0221(HIGOS): 27 September to 2 October 2002 with recurvature.

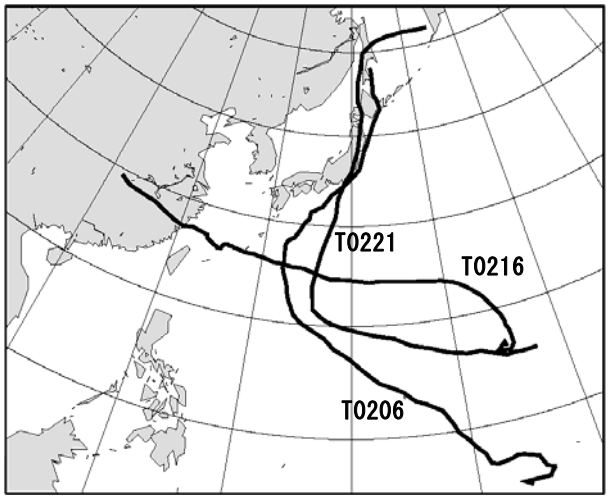


Fig. 1 Track of the target typhoons for the experiment. T0206 (CHATAAN), T0216 (SINLAKU), T0221(HIGOS).

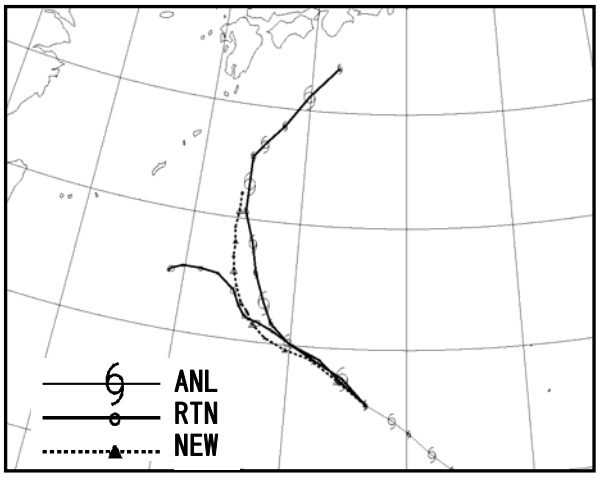


Fig. 2 Predicted track for the T0206 (CHATAAN) by TYM. (Initial time: 2002/07/06 00 UTC)
ANL: Analysis, RTN: Control, NEW: New TYM. Plotted every 6 hour.

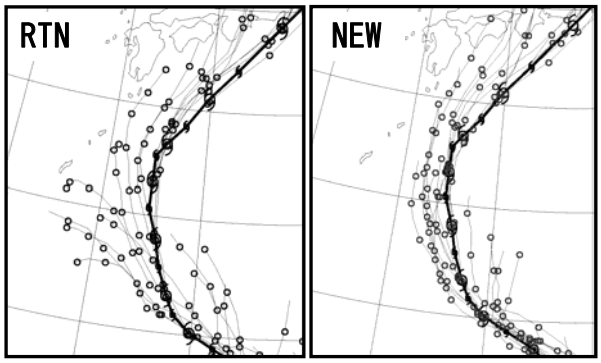


Fig. 3 Analyzed and predicted tracks around recurvature stage. The control (left panel) and the new TYM (right panel). Bold line is analyzed typhoon track. Thin lines are predicted typhoon track in each initial time. 6-hourly positions are plotted each line.

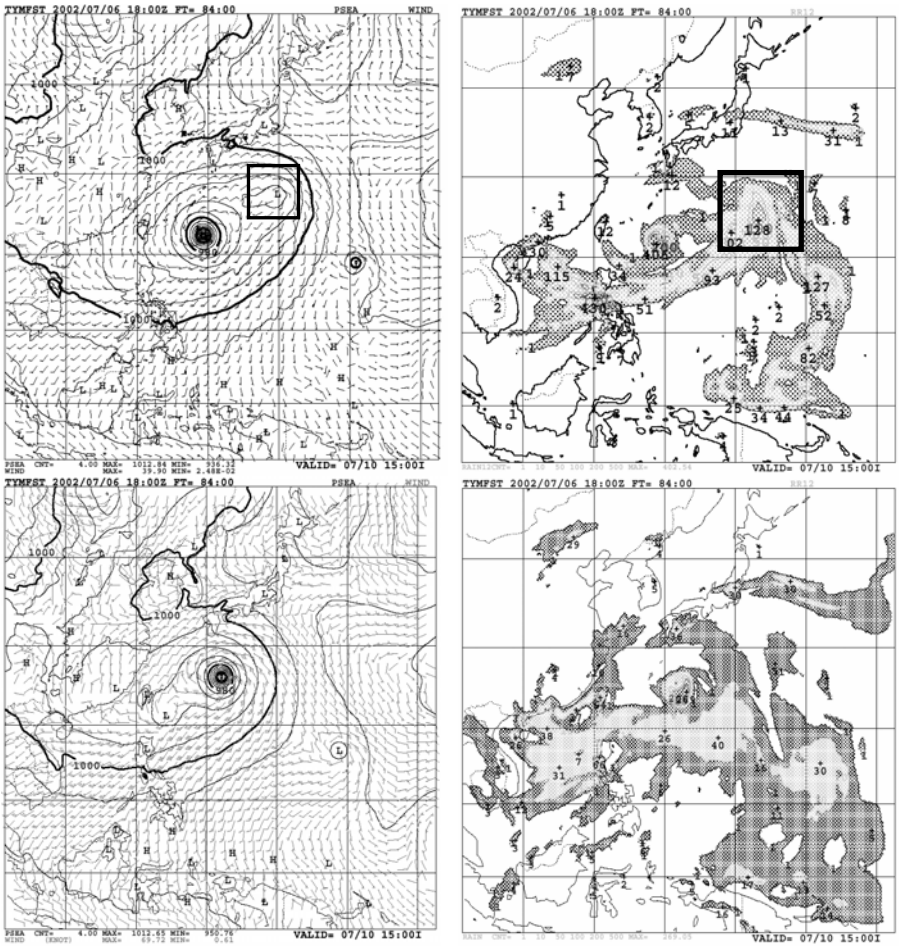


Fig. 4 84-hour forecast of the control (upper panels) and new (lower panels) TYMs. Initial time: 2002/07/06 18 UTC. Target typhoon: T0206 (CHATAAN). Mean sea level pressure (left panels) and 12-hour accumulated precipitations (right panels).

A false low and associated intensive precipitation are indicated with squares.

The operational TYM forecasts with the old physical process package are used as the control to evaluate the impact of the new physical processes.

Figure 2 shows the track for T0206 predicted by the new TYM starting from 00UTC 6 July 2002 along with those of the control and the analysis. In this forecast period, the typhoon changed its direction from north-westward to north-eastward (recurvature stage). In the control, the recurvature is not predicted and the typhoon continues to move to the northwest. In the case of the new TYM, though the moving speed is slower than the analysis, the recurvature is well predicted. Similar results are obtained from other forecasts starting from different initial times (Fig. 3). Figure 4 shows surface pressure and precipitation of the 84-hour forecast starting from 18UTC 6 July 2002. In the control, a small low and associated intensive precipitation are predicted to the northeast of the typhoon (between the sub-tropical high and the typhoon). The low moves to northeast along the western edge of the sub-tropical high following the anti-cyclonic flow.

The new TYM is superior to the control in the prediction of synoptic pattern in tropics. Figure 5 shows the 72-hour forecast for T0216 starting from 06UTC 2

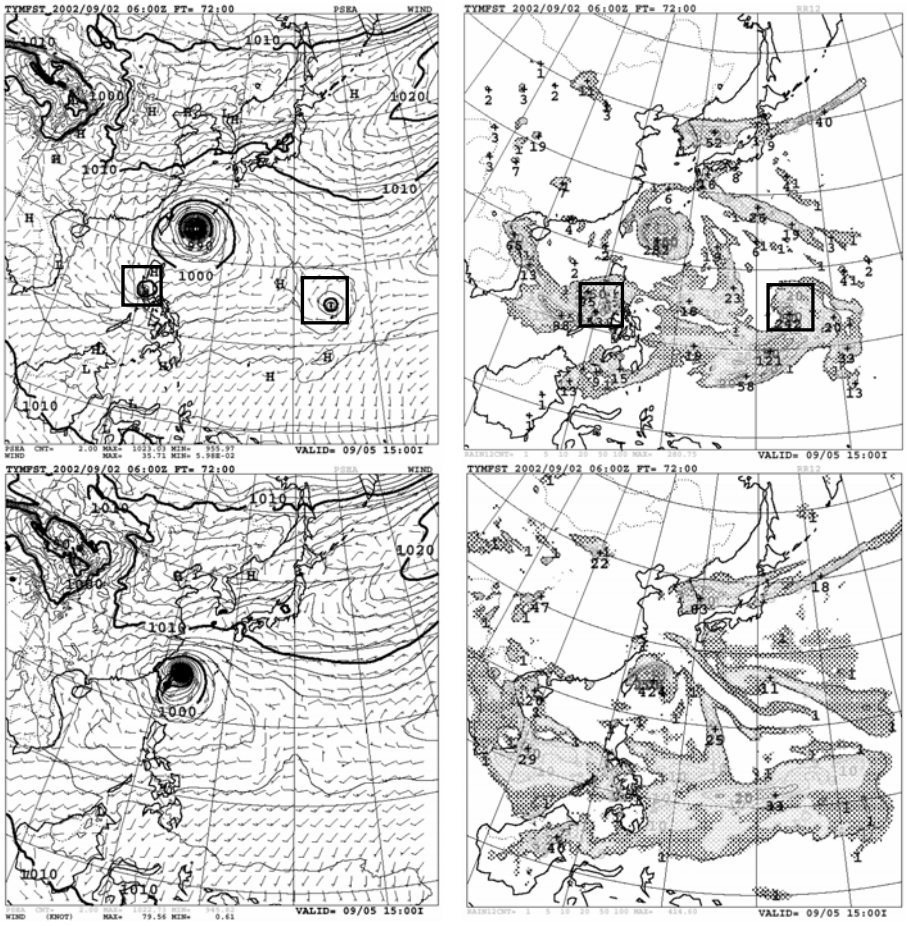


Fig. 5 72-hour forecast of the control (upper panels) and new (lower panels) TYMs. Initial times: 2002/09/02 06 UTC. Target typhoon : T0216 (SINLAKU). Mean sea level pressure (left panels) and 12-hour accumulated precipitations (right panels).
A false lows and associated intensive precipitation area are indicated with squares.

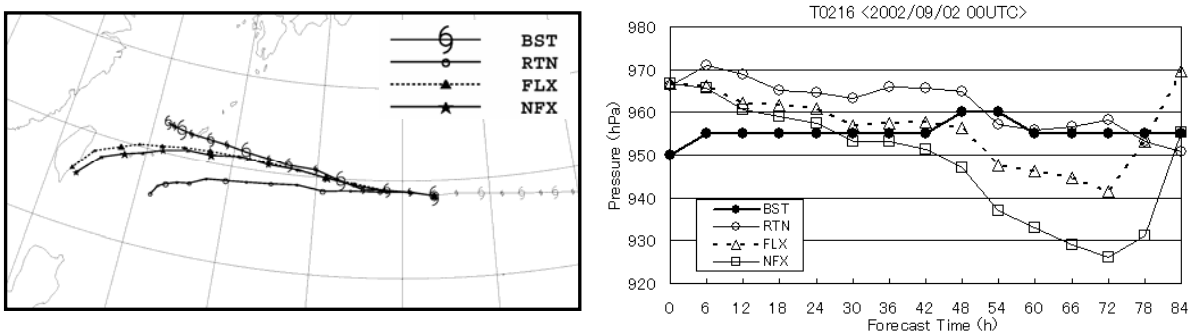


Fig. 6 Track (left panel) and intensity (right panel) forecast comparisons between the control and new TYM. Initial time: 2002/09/06 00UTC. Target typhoon: T0206 (CHATAAN).
ANL: Analysis, RTN: Control, NFX: Kondo(1975), FLX: Garratto (1992) and Beljaars(1995).
6-hourly intensity and position are plotted.

September 2002. Whereas intensive rain areas and small-scale lows are predicted around the Luzon Island and the Saipan Island in the control, these features are suppressed in the new TYM.

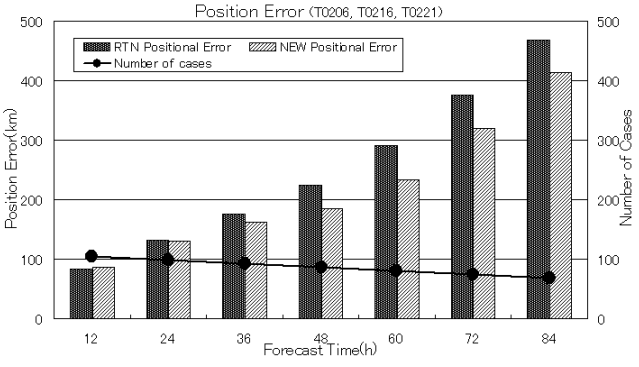


Fig. 7 Mean positional error of TYM.
Dark bar (RTN) is the control. Light bar (NEW) is the new TYM. Line is the number of cases.

Figure 6 shows the impact of the different roughness length formulae on the intensity forecast for T0216 using the physical process package of GSM9912. Both of the experiments improve the track forecast compared to the control. In the experiment using the old (Kondo) roughness length formulae (thin solid line), the predicted central pressure of the typhoon is about 30 hPa lower than that of the analysis. In the experiment using the new (Garratt and Beljaars) roughness length formulae (broken line), the overestimation is suppressed and the predicted central pressure is closer to the analysis.

The comparison of the mean positional error between the control and the new TYM is shown in Figure 7. A remarkable improvement in mean positional error is seen at the later stage of the forecast time. The mean positional error is reduced by 56 km in 72-hour forecast (74 cases). Figure 8 shows scatter diagrams of the typhoon positional error in 72-hour forecasts. The south-westward bias after the recurvature stage is slightly reduced. The dispersion of the positional error in the new TYM is smaller than that in the old one.

The mean error (ME) and the root mean square error (RMSE) of the typhoon central pressure forecasts are shown in Fig. 9. Though RMSE varies with the forecast time, the new TYM has almost the same performance in RMSE as the old TYM. ME is reduced at the early stage of the forecast time. ME of the new TYM scarcely varies (2–3 hPa) during the forecast period.

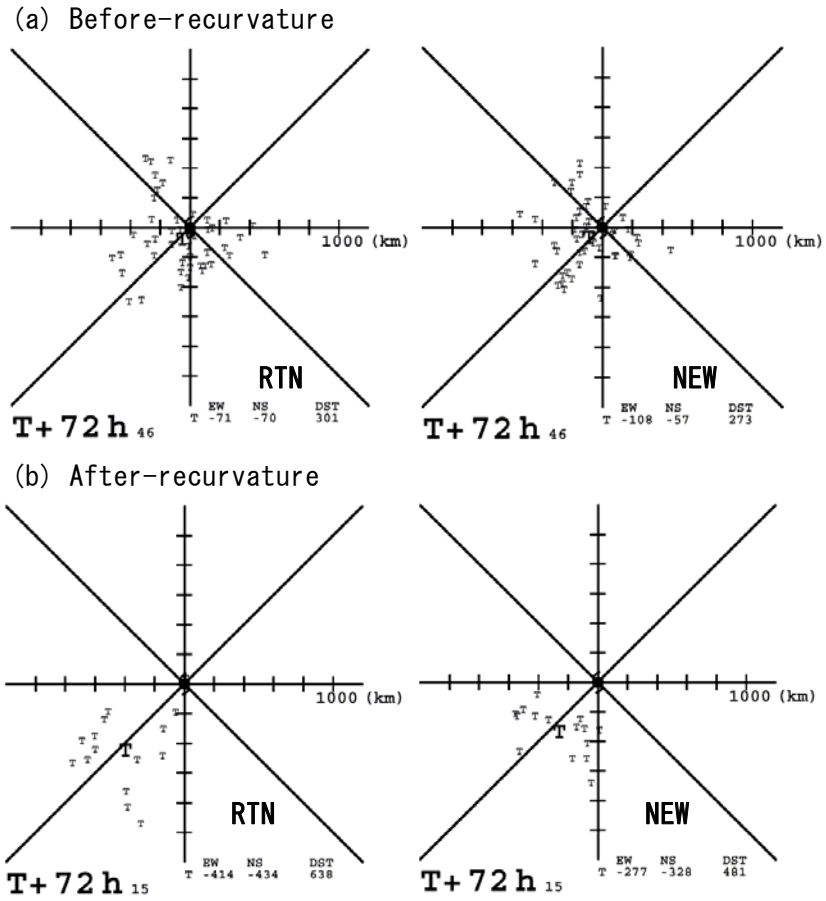


Fig. 8 Scatter diagram for 72-hour forecast error of typhoon position

The upper panels show the before-recurvature stage and the lower panels show the after-recurvature stage. The left panels show the control. The right panels show the new TYM. The predicted typhoon positions relative to the analysis are plotted. Up-direction shows the northward error and right-direction shows eastward error. Bold character '**T**' shows the mean positional bias.

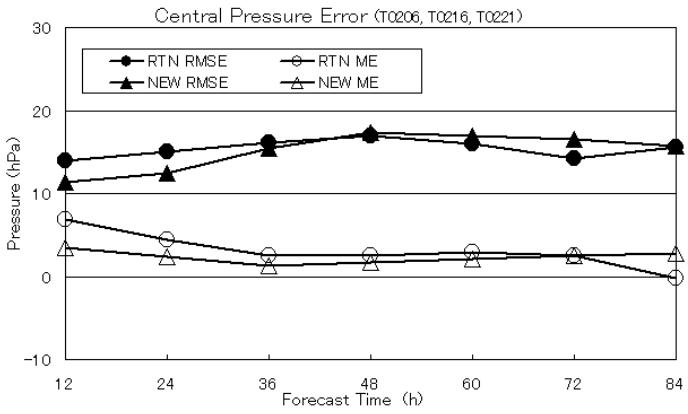


Fig. 9 Central pressure error of TYM.

RTN: control, NEW: new TYM. Black marks show root mean square error (RMSE). White marks show mean error (ME).

## 4. Summary

JMA has implemented a major version-up for TYM in July 2003. The version-up includes an introduction of precipitation and radiation processes based on those implemented in GSM in 1999. The roughness length formulae in calculating the heat (and water vapor) and momentum fluxes on the sea surface are also modified. False intensive rain areas associated with spurious small-scale lows in the tropics are suppressed. The typhoon track forecast is remarkably improved in the new TYM. As for typhoon intensity forecast, the new TYM produces almost same performance as the old one.

**[ APPENDIX ] The formulae of the roughness length on the sea surface in the new TYM**

The surface fluxes based on the Monin-Obukhov similarity theory are calculated with the following formulae :

$$\tau_x / \rho = -C_m |\mathbf{V}_a| u_a \qquad (1)$$

$$\tau_y / \rho = -C_m |\mathbf{V}_a| v_a \qquad (2)$$

$$H = -\rho c_p C_h |\mathbf{V}_a| (\theta_a - \theta_s) \qquad (3)$$

$$LE = -L\rho C_h |\mathbf{V}_a| (q_a - q_s) \qquad (4)$$

$$|\mathbf{V}_a| = \sqrt{u_a^2 + v_a^2}$$

where $\tau_x$ and $\tau_y$ are the momentum flux, $H$ the sensible heat flux, $LE$ the latent heat flux, $\theta$ the potential temperature, $q$ the specific humidity, $\rho$ the density of air, $C_p$ the heat capacity at constant pressure of the air, $L$ the latent heat of vaporization. Subscripts $a$ and $s$ denote the values at the lowest vertical level of the atmospheric model and the ground surface respectively. The exchange coefficient of momentum flux ($C_m$) and that of heat flux ($C_h$) proposed by Louis et al. (1981) are as follows:

$$C_m = \left\{ \frac{k}{\ln(z_a / z_{0m})} \right\}^2 \mathrm{fm}(Ri, z_a / z_{0m}) \qquad (5)$$

$$C_h = \frac{k}{\ln(z_a / z_{0m})} \frac{k}{\ln(z_a / z_{0h})} \mathrm{fh}(Ri, z_a / z_{0m}, z_a / z_{0h}) \qquad (6)$$

where $k$ is the von Karman's constant (=0.4), $z_{0m}$ the roughness length for momentum, $z_{0h}$ the roughness length for heat, $R_i$ the Richardson number, and fm and fh the functions decided by stability (Refer to JMA (2002) for the details). Different values of the roughness length are used for the land from that for the sea surface. Only the roughness length on the sea surface is changed in the experiments.

In the old TYM, the roughness length on the sea surface is calculated by following

formulae derived from Kondo (1975):

$$\begin{aligned} &u_{10} \le 25 m/s \\ &\quad z_0 = -34.7\times10^{-6} + 8.28\times10^{-4}u^* \\ &u_{10} > 25 m/s \\ &\quad z_0 = -0.227\times10^{-2} + 3.39\times10^{-3}u^* \end{aligned} \qquad (7)$$

where $u^*$ is a friction velocity and $u_{10}$ is a wind speed at 10 m height above sea level, $z_0$ is used for $z_{0m}$ and $z_{0h}$.

In the new TYM, the roughness length for momentum flux proposed by Beljaas (1995) and that for heat flux proposed by Garratt (1992) are used respectively:

$$z_{0m} = \frac{0.11\nu}{u^*} + \frac{\alpha}{g}u^{*2} \qquad (8)$$

$$z_{0h} = \exp\left\{-2.48\times\left(\frac{u^*\times z_{0m}}{\nu}\right)^{0.25} + 2.0\right\} \qquad (9)$$

where $\nu$ is the kinematic viscosity of air (=1.5x10$^{-5}$m$^2$/s), $g$ the acceleration of gravity and $\alpha$ = 0.018.

Emanuel (1995) indicates that the intensity of simulated tropical cyclones depends on the value of Ch/Cm. In the case of large values of Ch/Cm, the simulated typhoon is intensified, and vice versa. The value of Ch/Cm for the new TYM is smaller than that for the old one (Fig. A), and the overestimation of typhoon intensity is suppressed.

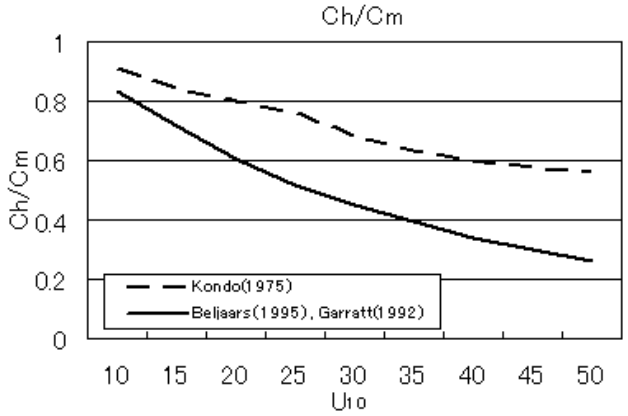


Fig. A The ratio of Ch to Cm, as a function of wind speed at 10m height. The ratio calculated under the stable condition at the surface boundary layer.

**Reference**


Bao, J. -W., S. A. Michelson, J. M. Wilczak, 2002: Sensitivity of numerical simulations to parameterizations of roughness for surface heat fluxes at high winds over the sea. *Mon. Wea. Rev.* **130**, 1926-1932.

Beljaars, A. C. M., 1995: The parameterization of surface fluxes in large-scale models under free convection. *Quart. J. Roy. Meteor. Soc.*, **121**, 255-270.

Emanuel, K. A., 1995: Sensitivity of tropical cyclones to surface exchange coefficients and a revised steady-state model incorporating eye dynamics. *J. Atmos. Sci.*, **52**, 3969-3976.

Garratt, J. R., 1992: The Atmospheric Boundary Layer. Cambridge University Press, 316pp.

Hosomi, T. 2002: Upgrading physical processes in the regional model. NWPP Report Series No. 28, Numerical Weather Prediction Progress Report for 2001. WMO/TD No.1151.

JMA, 2002: Outline of the operational numerical weather prediction at the Japan Meteorological Agency. Appendix to WMO Numerical Weather Prediction Progress Report, 157pp.

Kondo, J., 1975: Air-sea bulk transfer coefficients in diabatic conditions. *Bound. Layer Met.*, **9**, 91-112.

Kuma, K. H. Kitagawa, H. Mino, and M. Nagata, 2001: Impact of a recent major version-up of the Global Spectral Model (GSM) at JMA on tropical cyclone predictions. *RSMC Tokyo-Typhoon Center Technical Review*, **No.4**, 14-20.

Louis, J. F., M. Tiedtke, J. F. Geleyn, 1981: A short history of the operational PBL -parameterization at ECMWF. Workshop on Planetary Boundary Layer Parameterization 25-27 Nov. 1981, 59-79.

Sakai. R, H. Mino and M. Nagata, 2002: Verifications of tropical cyclone predictions of the new numerical models at JMA. *RSMC Tokyo-Typhoon Center Technical Review*, **No.5**, 1-18.

Smith, R. N. B., 1990: A scheme for predicting layer clouds and their water content in a general circulation model. *Quart. J. R. Meteor. Soc.*, **116**, 435-460.

# Development of a Cumulus Parameterization Scheme for the Operational Global Model at JMA

**Masayuki Nakagawa**
*Numerical Prediction Division, Japan Meteorological Agency*
**Akihiko Shimpo**
*Climate Prediction Division, Japan Meteorological Agency*

## 1. Introduction

The Japan Meteorological Agency (JMA) adopted a prognostic Arakawa-Schubert scheme (Arakawa and Schubert 1974; Moorthi and Suarez 1992; Randall and Pan 1993; Pan and Randall 1998) for cumulus parameterization in Global Spectral Model (GSM). JMA revised this scheme in March 2001 to include a reevaporation effect of the convective precipitation (GSM0103) with a view to improving its performance in the medium- to long-range predictions of tropical precipitation and associated circulation. Preliminary forecast experiments indicated that the GSM without the cooling and moistening effects of the reevaporation tended to produce stronger precipitation over the intertropical convergence zone as compared with observation and weaker one in the vicinity of the Philippines. This erroneous precipitation distribution was the main reason for poor medium- to long- range weather prediction of the GSM prior to the implementation of GSM0103. However, GSM0103 had a cold bias and an associated systematic error for geopotential height field in forecast at the lower troposphere over wide areas of the low latitudes especially in the summer hemisphere on early forecast days. The main reason for these errors was the excessive cooling by evaporating convective precipitation.

JMA has developed a new cumulus parameterization scheme which considers the detrainment effect in addition to the entrainment between the cloud top and the cloud base in convective downdraft and abolishes reevaporation of convective precipitation (GSM0305). This paper gives results of forecast/assimilation experiments to evaluate two versions of GSM.

## 2. Experiment setup

The model used in this paper is GSM with triangular truncation at the wave number 213. In the vertical, the model places 40 layers up to 0.4 hPa. For further details of GSM and the data assimilation system, see JMA (2002). The major differences between GSM0103 and GSM0305 are as follows:

(i) The cumulus parameterization scheme is upgraded to consider the detrainment effect in addition to the entrainment between the cloud top and the cloud base in convective downdraft and to abolish the reevaporation of convective precipitation.

(ii) The estimation of the moist static energy at the cloud base is changed from the sum of the average in the planetary boundary layer and the effect of turbulent flow to the maximum value in the planetary boundary layer.

(iii) The convective momentum transport scheme is revised to include the entrainment

and detrainment effects between the cloud top and the cloud base.

(iv) Time constants to reduce a cloud work function and to dissipate cumulus kinetic energy are shortened.

(v) The conversion rate from cloud water to precipitation in the large scale precipitation scheme is modified to consider the effect of convective rain.

In GSM0103, detrainment from a convective downdraft is assumed to occur only below the cloud base, whereas entrainment is assumed to occur between the cloud top and the cloud base. The effect of detrainment between the cloud top and the cloud base is considered in GSM0305 to represent convective downdraft which cools and moistens lower troposphere more realistically. At the same time, the reevaporation of convective precipitation is omitted because the evaporation of raindrop falling through humid air should be negligible.

The 3D-Var data assimilation system is also renewed. The raw ATOVS radiance data are directly assimilated in the new system instead of conventional retrieved thickness data (Kazumori et al. 2004). As a result, we can avoid errors due to retrieval and reflect moisture observations as well as temperature observations to the analysis. Regression coefficients and the background error covariance matrix in the 3D-Var assimilation system are also updated (Fujita 2004).

To test the impact of the new scheme, two forecast/assimilation experiments are conducted. One consists of GSM0103 and the old version of 3D-Var assimilation system (hereafter CNTL), while the other comprises GSM0305 and the new 3D-Var assimilation system (hereafter TEST). The periods for the experiments are from 28 June to 8 August 2002 and from 28 November 2001 to 8 January 2002. Nine days forecasts are performed for 31 initials of 12UTC 1-31 July 2002 and 1-31 December 2001 for both CNTL and TEST. The results are compared with each other.

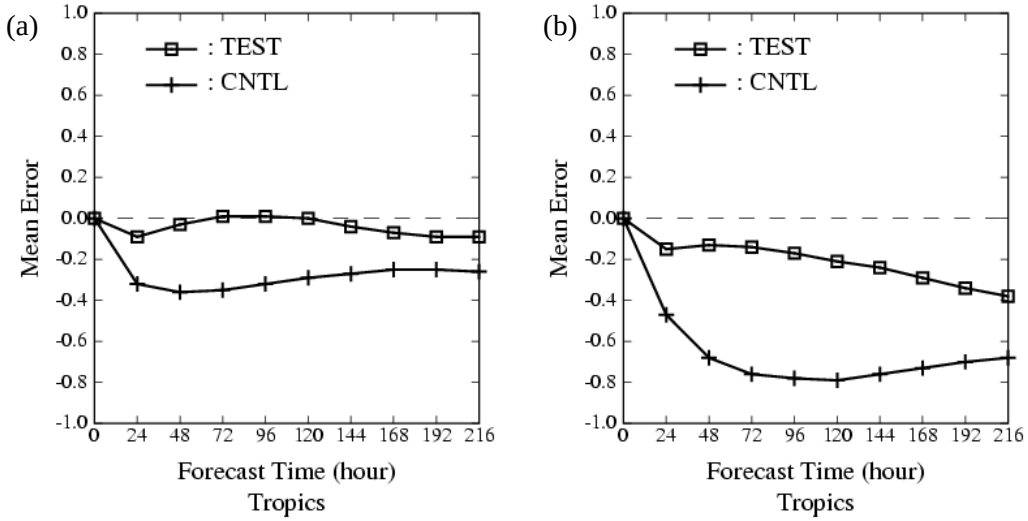


Fig. 1. Time series of the mean forecast error of 850 hPa temperature (K) over the tropical zone (20S - 20N) averaged over the 31 forecasts. (a): July 2002, (b): December 2001, +: CNTL, □: TEST.

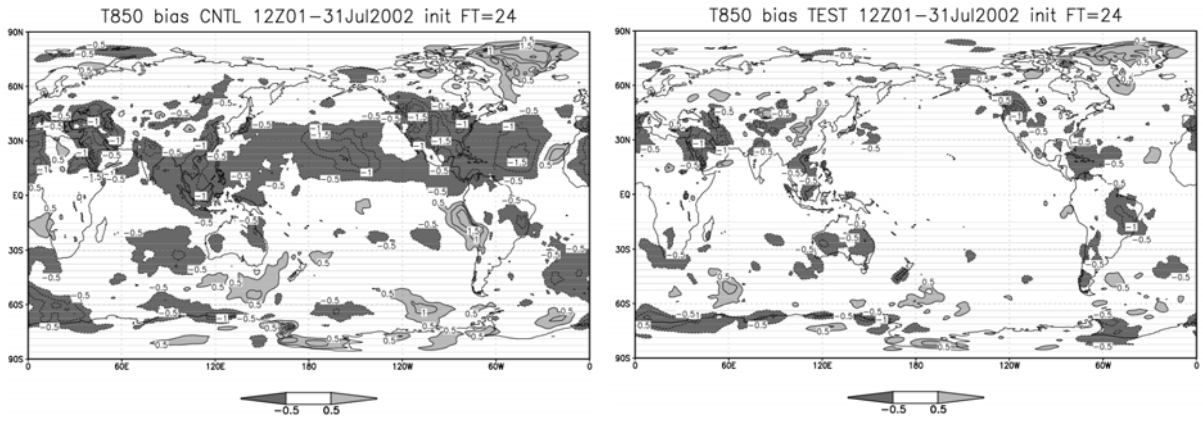


Fig. 2. Mean error of 24-hour forecast for 850 hPa temperature (K) averaged over the 31 forecasts in July 2002 by CNTL (left) and TEST (right). Areas with mean forecast errors larger than 0.5 K are lightly shaded and those less than –0.5 K are darkly shaded.

**3. Results**

Figure 1 shows the time series of the mean forecast error of 850 hPa temperature over the tropical zone (20S-20N) averaged over the 31 forecasts. It is seen that CNTL shows a systematic cold bias throughout the forecast periods both in July 2002 and December 2001 experiments. The bias is much smaller in TEST than in CNTL. This difference can be attributed to the change in the cumulus parameterization scheme. It is found that the heating rate by cumulus convection in the tropical zone at the lower troposphere of TEST forecast is larger than that of CNTL forecast, which can cause the reduction of bias. The tendency to predict the 500 hPa geopotential height field lower than the analysis field in CNTL is also reduced in TEST (not shown), which can be explained by the reduced cold temperature bias in the lower troposphere.

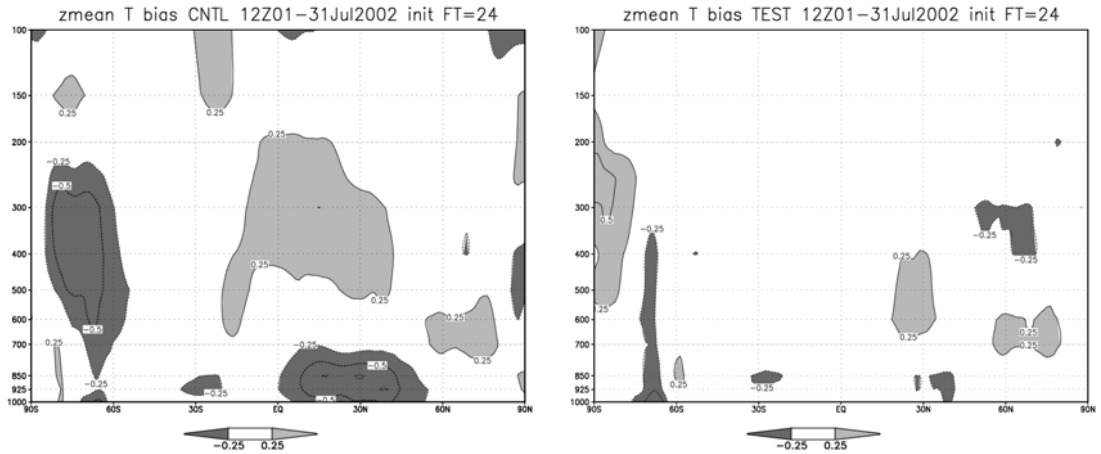


Fig. 3. Vertical cross sections of mean error in 24-hour forecast for the zonal mean temperature (K) averaged over the 31 forecasts in July 2002 by CNTL (left) and TEST (right). Areas with mean forecast errors larger than 0.25 K are lightly shaded and those less than –0.25 K are darkly shaded.

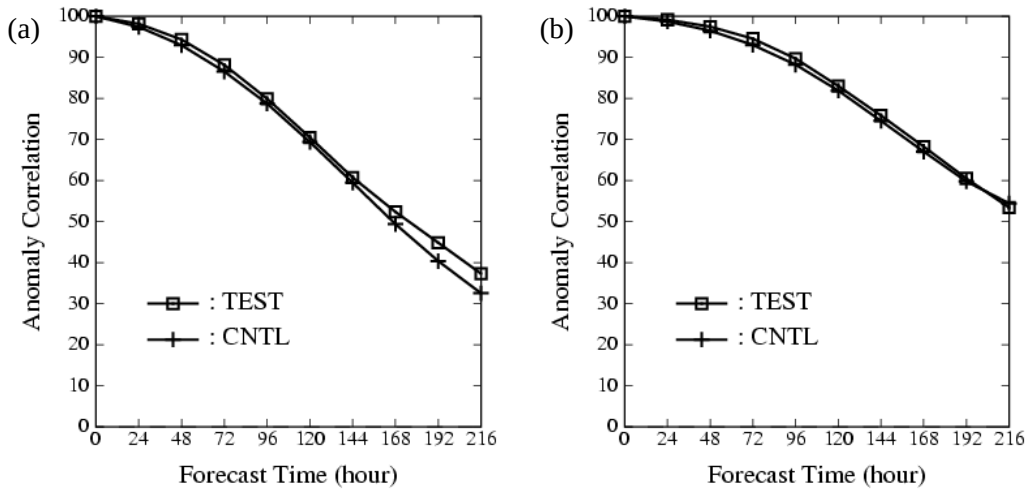


Fig. 4. Time series of the global anomaly correlation of 500 hPa geopotential height averaged over the 31 forecasts. (a): July 2002, (b): December 2001, +: CNTL, □: TEST.

The mean error of 24-hour forecast of 850 hPa temperature for July 2002 experiment is shown in Fig. 2. The area with cold bias lower than –0.5 K is shaded thick. The forecast field by CNTL is systematically lower than the analysis field on wide areas in the Northern (summer) Hemisphere. TEST produces much better forecasts than CNTL, which is consistent with the smaller temperature bias at lower troposphere as shown in Fig. 1.

Figure 3 shows the vertical cross sections of mean error in 24-hour forecast for the zonal mean temperature averaged over 31 forecasts in July 2002. In the low latitudes, CNTL shows cold bias at the lower troposphere and warm bias at the middle troposphere, whereas the bias of TEST is smaller.

Anomaly correlation of 500 hPa geopotential height forecast is shown in Fig. 4. It is seen that the impact of the new convection scheme and data assimilation system is positive in both July 2002 and December 2001 experiments. To separate the impact of the new convection scheme from that of the new data assimilation system, a preliminary experiment using the new convection scheme and the old data assimilation system is conducted with the exception that the ATOVS channels sensitive to the moisture is directly assimilated. Heating rate by the cumulus convection in the tropical zone at the lower troposphere of GSM0305 forecast is larger than that of GSM0103 forecast, which results in the reduction of the forecast bias at the lower troposphere. In contrast, the anomaly correlation shows almost no improvement. These results suggest that the improvement seen in Fig. 2 is due to the new convection scheme and that seen in Fig. 4 may be attributed to the direct assimilation of the ATOVS channels sensitive to the temperature field.

It is expected that the improvement in forecast for the tropics leads the better performance in the typhoon track prediction. Figure 5 shows the forecast tracks of typhoon Halong (0207) by CNTL and TEST along with the best track analyzed by the RSMC Tokyo – Typhoon Center. It is seen that CNTL track shows northeastward error. This error may be caused by the tendency to predict the subtropical anticyclone weaker, which is related to the

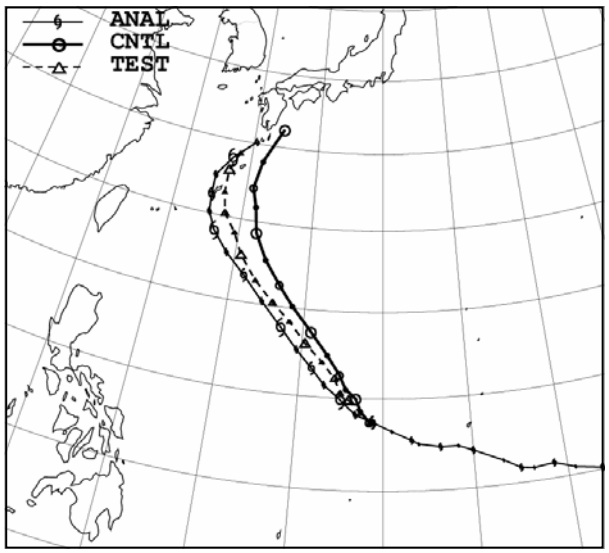


Fig. 5. Tracks of Typhoon Halong (0207) predicted by CNTL (thick line with circle) and TEST (broken line with triangle) at 12 UTC 11 July 2002. Analyzed best track (ANAL) is plotted by a thin line with section marks.

systematic negative error in forecast of the geopotential height field at the lower troposphere. TEST makes a much better forecast than CNTL, which is consistent with the smaller bias of the geopotential height field.

**4. Summary**

JMA has developed a new cumulus parameterization scheme in order to reduce the cold bias and associated negative bias for the geopotential height field in forecast at the lower troposphere. The data assimilation system is also renewed.

Forecast/assimilation experiments are conducted to test the impact of the new convection scheme and data assimilation system. The bias apparent in forecast of CNTL is substantially reduced in TEST. This improvement can be attributed to the change of the cumulus parameterization scheme. The anomaly correlation of the TEST forecast for the 500 hPa geopotential height field is higher than the CNTL forecast.

Typhoon track prediction is improved significantly by TEST in several cases as compared with CNTL. This improvement in TEST is explained by the reduction of the systematic negative error apparent in the CNTL forecast for the geopotential height field at the lower troposphere.

It is clear that the new cumulus parameterization scheme suppresses the systematic error of GSM0103 in temperature and geopotential height fields at lower troposphere. JMA implemented in May 2003 the new convection scheme and the 3D-Var data assimilation system with the direct assimilation of ATOVS radiance data in the operational GSM.

**References**

Arakawa, A. and W. H. Schubert, 1974: Interaction of a cumulus cloud ensemble with the large-scale environment, Part I. *J. Atmos. Sci.*, *31*, 674-701.

Fujita, T., 2004: Revision of the Background Error Covariance in the Global 3D-Var Data Assimilation System. Submitted to the 2004 Research Activities in Atmospheric and Oceanic Modelling, CAS/JSC Working Group on Numerical Experimentation.

JMA, 2002: Outline of the operational numerical weather prediction at the Japan Meteorological Agency. Appendix to WMO Numerical weather prediction progress report.

Kazumori, H., H. Owada and K. Okamoto, 2004: Improvements of ATOVS radiance-bias correction scheme at JMA. Submitted to the 2004 Research Activities in Atmospheric and Oceanic Modelling, CAS/JSC Working Group on Numerical Experimentation.

Moorthi, S. and M. J. Suarez, 1992: Relaxed Arakawa-Schubert: A parameterization of moist convection for general circulation models. *Mon. Wea. Rev., 120*, 978-1002.

Pan, D.-M. and D. Randall, 1998: A cumulus parameterization with a prognostic closure. *Quart. J. Roy. Meteor. Soc., 124*, 949-981.

Randall, D. and D.-M. Pan, 1993: Implementation of the Arakawa-Schubert cumulus parameterization with a prognostic closure. Meteorological Monograph/The representation of cumulus convection in numerical models. *J. Atmos. Sci., 46*, 137-144.

# Operational use of ATOVS radiances in global data assimilation at JMA

**Masahiro Kazumori, Kozo Okamoto, Hiromi Owada**
*Numerical Prediction Division, Japan Meteorological Agency*

## 1. Introduction

The Advanced TIROS Operational Vertical Sounder (ATOVS) radiances have been operationally assimilated in the Japan Meteorological Agency (JMA) global 3D-Var data assimilation system since 28 May 2003. It replaced TOVS/ATOVS retrievals, which had been assimilated in the JMA global data assimilation system. The direct assimilation of ATOVS radiances is superior to its retrieval assimilation because the retrievals have some error in their conversion from radiance to analysis variables such as temperature and relative humidity.

Data assimilation experiments, which was conducted before the operational use of ATOVS radiances demonstrated significant impacts on forecasts and analyses.

This report describes the ATOVS data used at JMA and some results of the assimilation experiments.

## 2. ATOVS

ATOVS instruments are sensors on the National Oceanic and Atmospheric Administration (NOAA) series of polar-orbiting satellites. ATOVS instruments are composed of three independent sensors; a High-resolution Infra-Red Sounder (HIRS) which has 20 channels and two Advanced Microwave Sounder Units (AMSU-A, AMSU-B) which have 15 and 5 channels, respectively. HIRS and AMSU-A measure mainly temperature profile and AMSU-B measures moisture profile. National Environmental Satellite and Data Information System (NESDIS) produces ATOVS radiance data (HIRS and AMSU-A) and thinned AMSU-B radiance data. These data are pre-processed Level 1D data (Reale 2001) and have temperature and moisture retrievals. In the previous retrieval assimilation, temperature was converted to thickness and then assimilated in 3D-Var. In the current direct assimilation, HIRS, AMSU-A and AMSU-B radiances are assimilated directly.

The Level 1D data undergo a re-mapping procedure in which AMSU-A field of view (FOV) is interpolated into HIRS FOV by NESDIS and has the cloud flag and the skin temperature. In addition, these data are thinned at 250km resolution in equal distance in a preprocess step of the JMA data quality control system. As for AMSU-B, the data are selected at 180km resolution. These distances are kept constant for all over the globe. Figure 1 shows comparison of data coverage used in the previous retrieval assimilation and the current radiance assimilation. The ATOVS data on land are assimilated in current direct assimilation system. However, AMSU-A channels 1-3 (all the globe) are not used because these channels observe surface conditions. AMSU-A channels 4-5 are not used over land. AMSU-A channel 6 and channel 7 are not assimilated if the elevation of observation point is over 1,500 meter and 2,500 meter, respectively. No land data had been used in previous retrieval assimilation. As for moisture data, GMS moisture data, which was retrieved from GMS radiance

statistically, had been assimilated jointly in the previous retrieval assimilation. Instead of the GMS moisture data, AMSU-B radiances are assimilated in the direct assimilation system.

Cloud contaminated data are rejected by a cloud cost method based on AAPP procedure (Okamoto et. al. 2002) because an accuracy of radiative transfer model (RTTOV-6, Saunders, 1998; Saunders, 2000) are degraded by cloud and rain presence. The surface type (sea, land or coast) is defined by 0.25-degree land mask data set. Coastal data are not used. Identification of sea ice is based on the JMA sea surface temperature analysis: an area where SST< 274.15K is regarded as sea ice.

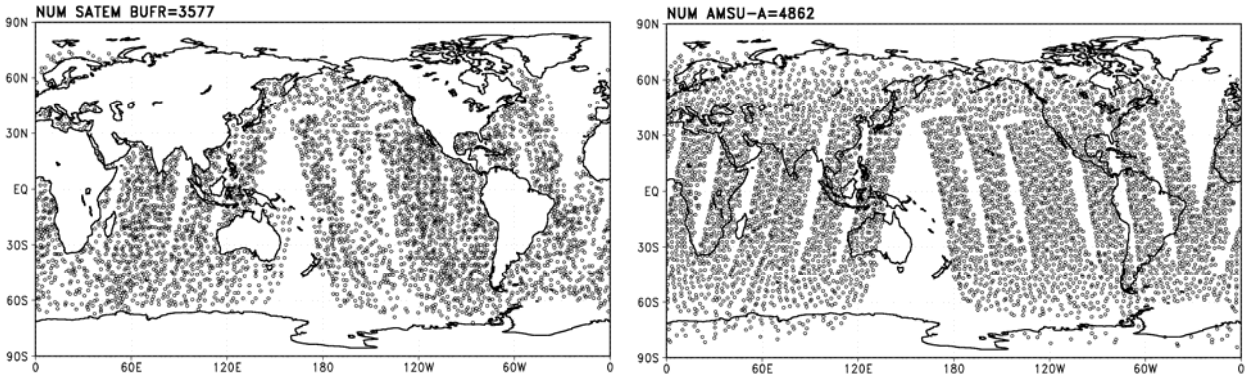


Fig. 1: Data coverage in a six-hour assimilation time from ATOVS instruments on NOAA15 and NOAA16 satellites. Left panel is for retrieval assimilation (500 hPa geopotential). Right panel is for direct assimilation (AMSU-A channel 6).

In order to use radiances from ATOVS, biases between observed radiances and simulated ones from first guess must be corrected. The JMA scheme for ATOVS radiance-bias correction relies on the total column water vapor from first-guess, the JMA SST analysis, and the calculated brightness temperatures from AMSU-A channels 5,7 and 10. They are used as linear predictors of the bias for each channel. The biases are removed before assimilation with 3D-Var.

**3. Design of experiments**

Data assimilation experiments were carried out for two periods: 27 June 2002 – 9 August 2002, and 27 November 2001 – 9 January 2002. Data configurations of the experiments were:

- Retrieval assimilation (CNTL)
- Direct assimilation + (new cumulus parameterization scheme) + (new background-error covariance) (TEST)

No use of ATOVS retrievals and relative humidity profile retrieved from GMS-5 brightness temperature in the TEST.

In these experiments, the JMA Global Spectral Model (GSM) at resolution T213L40 and the 3D-Var assimilation system were used. ATOVS data from NOAA15 (AMSU-A, AMSU-B) and NOAA16 (HIRS, AMSU-A and AMSU-B) were used. Moreover a new cumulus parameterization scheme of the global model and a new 3D-Var background-error

covariance were jointly used for TEST. In the TEST, ATOVS moisture channels, i.e. HIRS channel 10,11 and 12 and AMSU-B channel 3, 4, and 5 were assimilated instead of retrieved relative humidity profile from the GMS-5 brightness temperature.

## 4. Results

As for temperature field, large impact was found in the upper stratosphere from 30 hPa to 0.4 hPa. Figure 2 show the monthly zonal mean temperature for July 2002. By using radiances directly, profile of temperature became smooth. Figure 3 shows a verification of analyzed temperature and first-guess temperature against radiosonde observation. Better fits were found in the troposphere and lower stratosphere in the TEST.

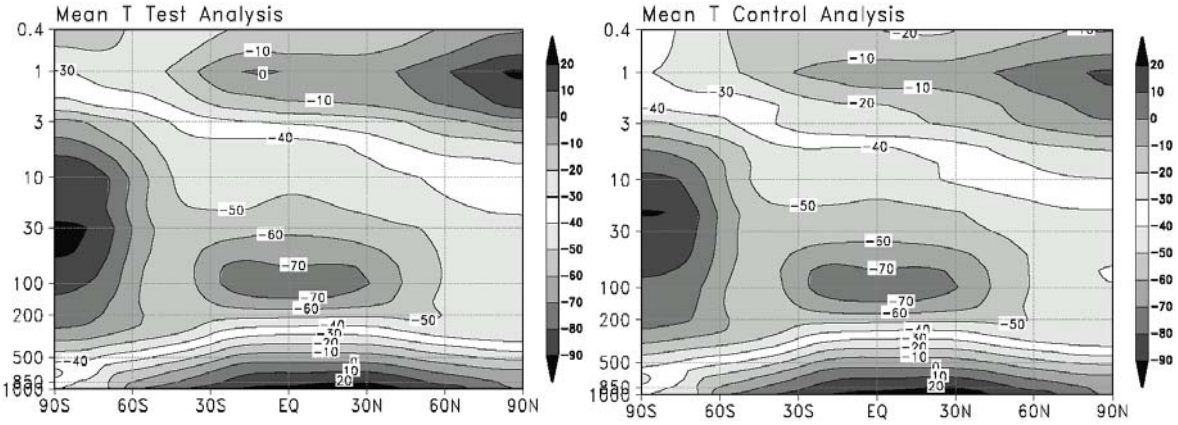


Fig. 2: Zonal mean of temperature in the experiments averaged over July 2002. The left panel is TEST and the right panel is CNTL. The contour interval is 10K.

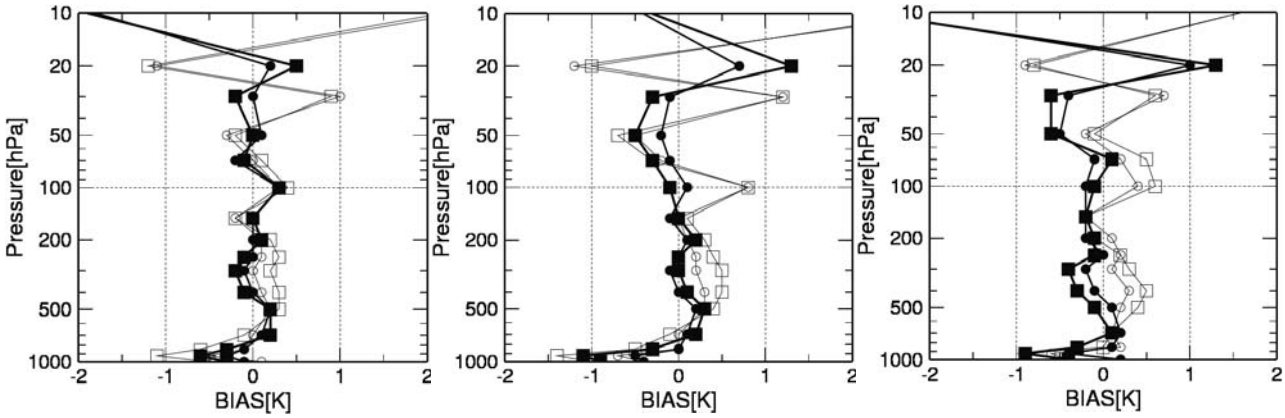


Fig. 3: Mean difference of the first guess (TEST: ○, CNTL: □) and the analyzed fields (TEST: ●, CNTL: ■) from radiosonde temperature observations for July 2002. The left panel is the Northern Hemisphere (90°N-20°N), the middle panel is the tropics (20°N-20°S), and the right panel is the Southern Hemisphere (20°S-90°S).

Figure 4 shows a difference between analyzed total precipitable water and SSM/I retrieval. Because SSM/I data are not assimilated, they are independent data. The upper panel is the

difference for TEST and the lower panel is that for CNTL for 15 July 2002. In the TEST case, the difference became small in tropical region. This result indicates that humidity field became realistic by assimilating ATOVS moisture channels.

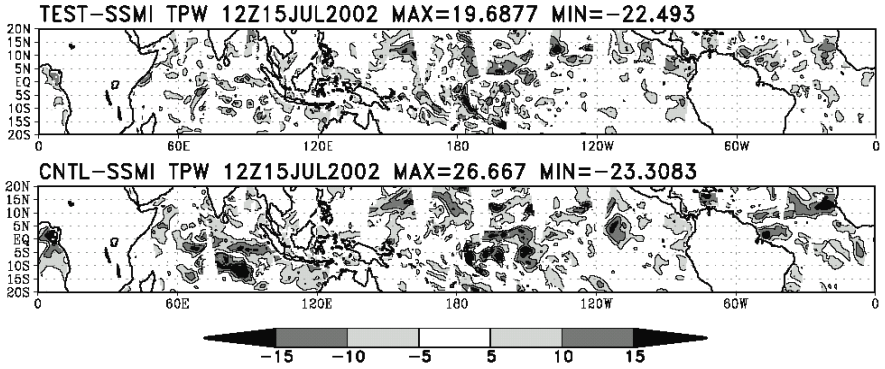


Fig. 4: Difference between analyzed total precipitable water and that retrieved from SSM/I observations for 12UTC 15 July 2003. The upper panel is TEST-SSM/I, and the lower panel is CNTL-SSM/I. The contour interval is 5mm.

As for impact on forecast, the TEST run has demonstrated positive impacts for the geopotential height at 500 hPa (Fig 5). Particularly, substantial positive impacts were found in the Southern Hemisphere and in the tropical region. Figure 6 shows a monthly mean difference between RMSE of 24-hour forecasts from TEST and those from CNTL. The negative value means positive impact. Obviously, the positive impact on forecasts in the Southern Hemisphere is larger than other area.

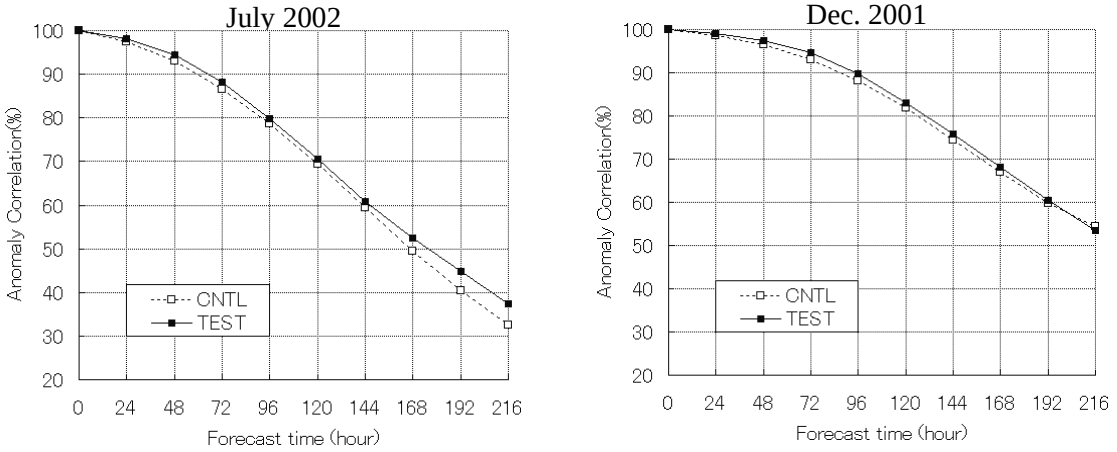


Fig. 5: Mean anomaly correlations for 500hPa geopotential height over the globe. The left panel is for July 2002 and the right panel is for December 2001. Each score is calculated by averaging 31 cases.

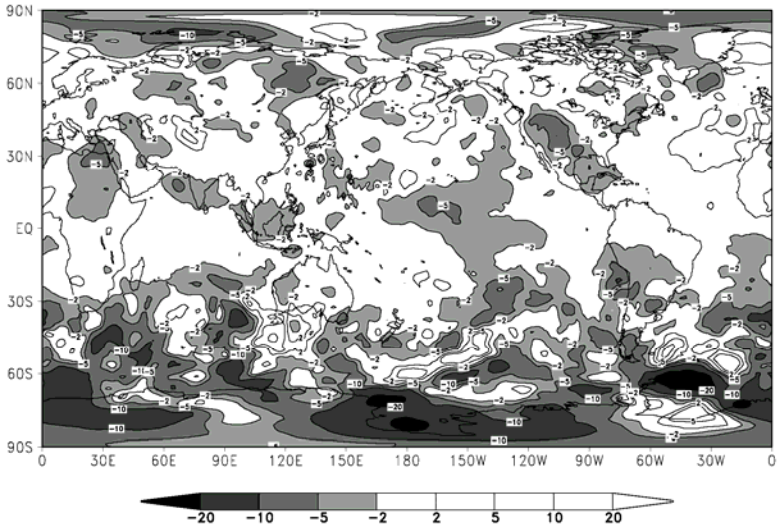


Fig. 6: Monthly mean difference of RMSEs between TEST and CNTL 24-hour forecasts for July 2002. Negative value (Gray color) shows positive impact.

The TEST forecast scores of temperature at 850 hPa, wind speed at 250 hPa and sea level pressure were similarly higher than CNTL.

Positive impacts were also found in prediction of the typhoon tracks. Figure 7 is a comparison of typhoon track prediction between TEST forecast and CNTL forecast. Because the underestimation in the forecast of strength of the subtropic high pressure was reduced, the typhoon track prediction was corrected westward. Similar position impacts for other typhoon events were also found.

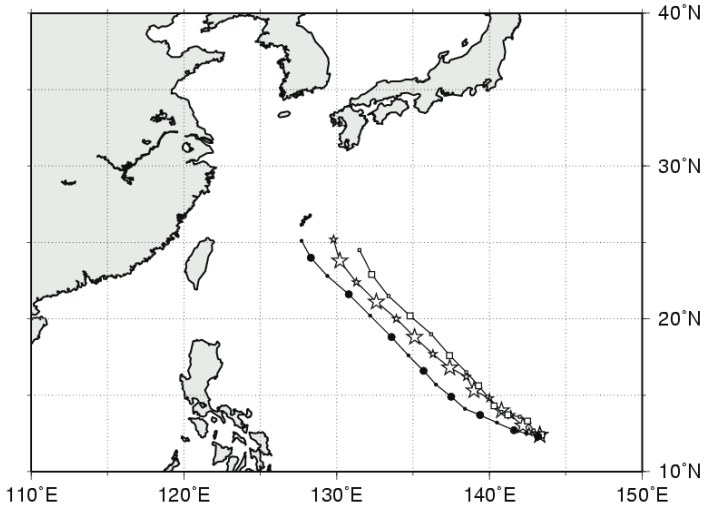


Fig. 7: A comparison of typhoon T0207 (HALONG) track prediction. Initial time is 12UTC 10 July 2002. ●:Best Track, ☆:TEST, □:CNTL.

**5. Summary and Future prospect**

JMA has started operational use of ATOVS radiances in the global data assimilation on 28

May 2003. The use of ATOVS retrievals and GMS-5 retrievals was discontinued. Experiments prior to the operational use have demonstrated dramatic positive impacts. The temperature profiles in the upper stratosphere and the global humidity fields in the troposphere were improved. The higher accuracy of initial fields of temperature and humidity were confirmed by comparing with radiosonde observations and the total precipitable water estimated from SSM/I. As for forecast skill, positive impacts were found for the geopotential height at 500 hPa in the Southern Hemisphere and in the tropical region. The improvement in short-range forecast was remarkable. Moreover better results on the typhoon track prediction were also found.

The direct assimilation of ATOVS data expanded moisture observation coverage and improved the quality of temperature and humidity analysis. Then, direct assimilation led to higher performance of the prediction globally. JMA has achieved considerable progress in ATOVS data assimilation, but some unpreferable changes in temperature analysis are seen at some levels in the stratosphere and the excessive concentration of rainfall in 6-hour forecast is also seen in the tropics. To solve these problems, we continue to improve the bias correction scheme of ATOVS brightness temperature. Moreover, we are going to assimilate ATOVS Level 1B data to avoid intrinsic errors in the level 1D data. And we have a plan to update the radiative transfer model from RTTOV-6 to RTTOV-7.

**References**

Okamoto, K. Takeuchi Y., Kaido Y., and Kazumori M. 2002. Recent Developments in assimilation of ATOVS at JMA. *Proceedings of 12th International TOVS Study Conference, Lorne, Australia.*

Reale, A. 2001: NOAA operational sounding products from advanced-TOVS Polar Orbiting Environmental Satellites, NOAA Technical Report NESDIS **102**, U.S. Dept. of Commerce, Washington D.C.

Saunders, R., M. Matricardi and P. Brunel 1998. An improved fast radiative transfer model for assimilation of satellite radiance observations. *Q. J. R. Meteorol. Soc.*, **125**, 1407-1425.

Saunders, 2000: Rttov-6 Science And Validation Report 2000.
http://www.met-office.gov.uk/research/interproj/ nwpsaf/rtm/old/d81svr.pdf

# Assimilation of QuikSCAT/SeaWinds Ocean Surface Wind Data into the JMA Global Data Assimilation System

**Yasuaki Ohhashi**
*Numerical Prediction Division, Japan Meteorological Agency*

## 1. Introduction

A satellite-borne scatterometer obtains the surface wind vectors over the ocean by measuring the radar signal returned from the sea surface. It provides valuable information such as a typhoon center for numerical weather prediction (NWP) over the ocean, where conventional in situ observations are sparse. Observational data from the European Remote-Sensing Satellite 2 (ERS2) /Active Microwave Instrument (AMI) scatterometer launched by the European Space Agency (ESA) was used operationally at the Japan Meteorological Agency (JMA) from July 1998 to January 2001. A new scatterometer named SeaWinds was launched onboard the QuikSCAT satellite by the National Aeronautics and Space Administration (NASA)/Jet Propulsion Laboratory (JPL) on 19 June 1999. It was a “quick recovery” mission to fill the gap created by the loss of data from the NASA Scatterometer (NSCAT), when the Japanese Advanced Earth Observation Satellite (ADEOS) lost power in June 1997. The width of swath of QuikSCAT/SeaWinds is 1800 km, which is wider than that of ERS2/AMI by three times, with a spatial resolution of 25 km. Daily coverage is more than 90% of the global ice-free oceans.

Figure 1 shows an example of QuikSCAT/SeaWinds observation. The QuikSCAT/SeaWinds observes with higher density than ship or buoy. A cyclonic

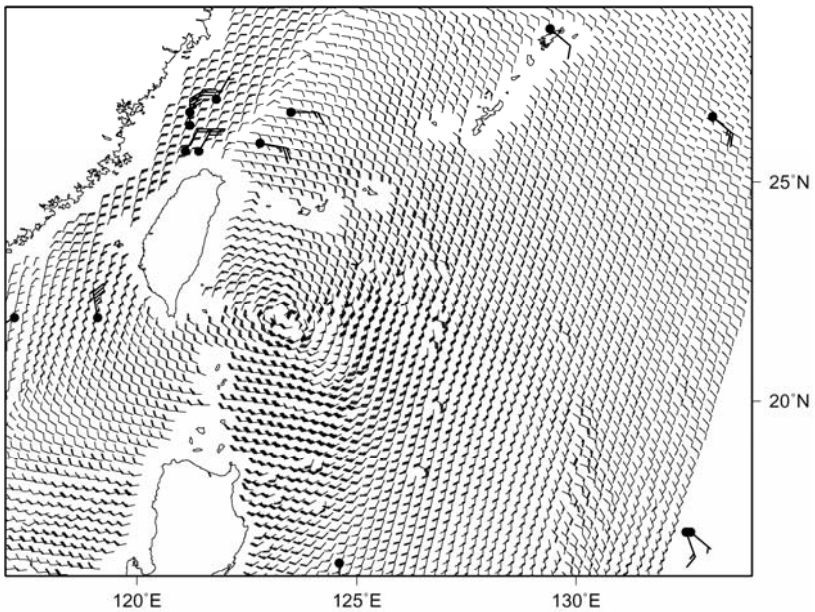


Fig.1 Wind data around typhoon T0306 (SOUDELOR) observed by QuikSCAT/SeaWinds. Observation time is about 10 UTC 17 June 2003. A full wind barb is 10 knots and a half wind barb is 5 knots. Observations by ships are plotted as dots with large barbs.

circulation around the center of a typhoon is apparent.

In section 2, a quality control system for SeaWinds data is described. In section 3, results from data assimilation experiments are presented. In section 4, conclusions and future plans of assimilation of scatterometer data are provided.

## 2. Quality control system for scatterometer data

In order to assimilate scatterometer data effectively, a quality control system for SeaWinds data (Tahara 2000) was built up (Fig.2). The QuikSCAT/SeaWinds Operational Standard Data Product (Level 2.0B(L2B)) from the National Oceanic and Atmospheric Administration (NOAA)/National Environmental Satellite Data and Information Service (NESDIS) (Leidner et al. 2000) is received at JMA in near real-time. First, the low quality data over land or sea ice are rejected. Because the data in heavy rain areas have less accuracy due to scatter noises by rain drops, the data flagged as rain (Huddleston and Stiles 2000) are rejected. The next is the ambiguity removal step. The wind retrieval process from original backscattered cross section data produces a set of 2 to 4 potential wind vector solutions (known as “ambiguities”). Those ambiguity vectors have nearly the same speed, but quite different wind directions. To determine the most likely wind vector, NWP nudging technique which chooses the vector closest to the first guess wind and median filter technique which selects the vector similar to adjacent data are used. Then wind speed check and wind direction check are performed. In the wind direction check step, a QC scheme called “Group QC” is introduced. The conventional QC occasionally rejects correct wind data in and around severe weather systems such as cyclones and fronts, because wind direction and speed varies sharply there and the difference between the first guess field and observations tends to be large. The group QC

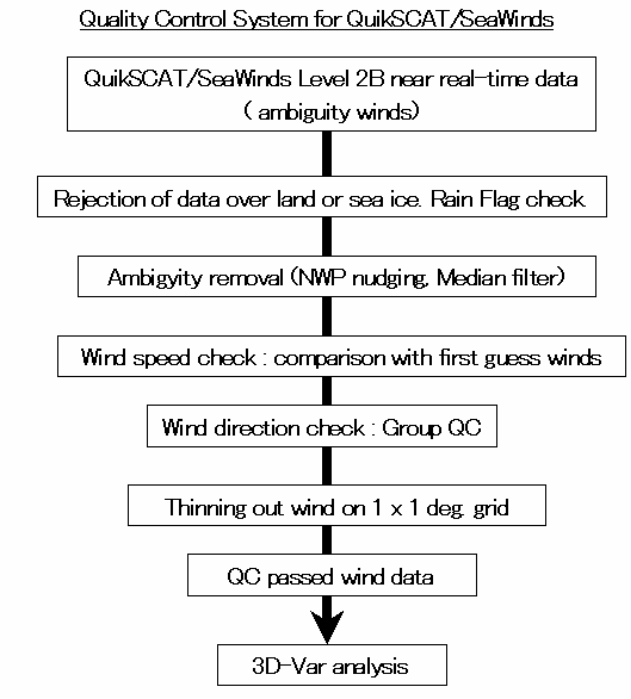


Fig.2 Quality control procedure for QuikSCAT/SeaWinds data.

is a technique to save those important data. It consists of two steps. The first is a grouping step, in which scatterometer data are divided into some groups consisting of adjacent data which have the similar wind directions and speeds. The next is a testing step, in which the data are checked group by group against the first guess field. Correct data which would be rejected by the conventional QC are saved by comparing with surrounding correct data. The group QC saves a lot of correct scatterometer data in and around severe weather systems successfully. Finally wind data are thinned on 1 x 1 degree (lat./lon.) grid and used in the data assimilation procedure.

## 3. Impact study for SeaWinds data

Data assimilation experiments of SeaWinds were conducted using the T213L40 version of the JMA global model (GSM0103; JMA 2002) for December 2001 and July 2002. Data assimilation was started from 00 UTC 1 December 2001 (1 July 2002) and continued to 18 UTC 31 December 2001 (31 July 2002). Nine days forecasts started from 12 UTC analysis have been carried out for the period from 8 December (8 July) to 22 December (22 July). In the experiment for July 2002, relative humidity profiles retrieved from the GMS-5 brightness temperature were not used. Experiments with and without SeaWinds data are referred to as Test run and Control run, respectively.

### (1) SeaWinds wind data

Ebuchi et al. (2002) compared SeaWinds L2B data with buoys. They indicated that the root-mean-squared differences of the wind speed and direction were about 1 m/s and 23°, respectively, with no systematic biases.

After the QC procedure, SeaWinds data were compared with first guess wind fields. The results showed that RMSE and BIAS in wind speed were 1.91 m/s and 0.81 m/s in December, and 1.87 m/s and 0.66 m/s, respectively, in July. RMSE in wind direction were 20.2° in December and 19.7° in July. Because those BIASs are similar to those between buoy data and first guess, the SeaWinds wind data have good accuracy enough to be used in NWP. Numbers of SeaWinds data which pass QC (Fig.2) in the cycle analysis and the early analysis[1] are about 10,000 and 6,000, respectively.

### (2) Impact on analysis

Figure 3 shows the impact of the SeaWinds wind data on the analysis fields. Using the SeaWinds data, the increment from the first guess field was up to 4 m/s (Fig.3(a)). The impact of SeaWinds data is also seen in the difference between the analysis field in Test and that in Control (Test－Control) (Fig.3(b)). The result shows that the analysis field of surface wind and that of sea surface pressure were changed mainly over SeaWinds observation areas. It is apparent that a cyclonic circulation was intensified and sea level pressure was decreased over 45°S-55°S and 120°W-135°W by SeaWinds data

[1] The JMA global 3D-Var operational assimilation system consists of cycle analysis conducted four times a day (00,06,12,18 UTC) with longer data cut off times and early analysis for the GSM forecasts (00,12 UTC).

assimilation.

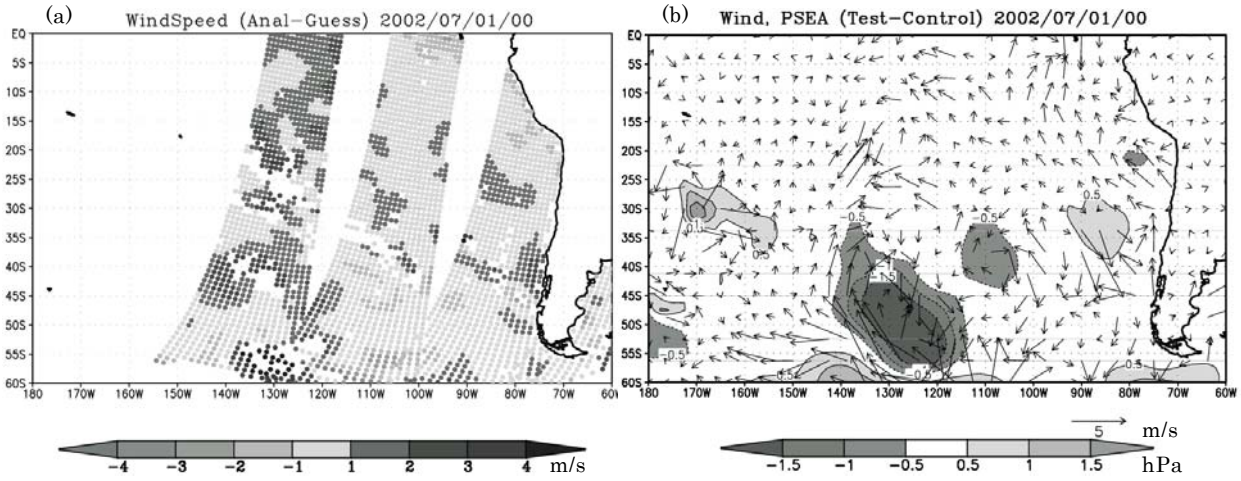


Fig.3 Impact of SeaWinds data on analysis fields at 00 UTC 1 July 2002. (a) Increment of sea surface wind speed (m/s) (Analysis－First guess). (b) Differences of analysis (Test－Control) of sea surface wind vectors (m/s) and sea level pressure (hPa).

**(3) Impact on forecasts**

Impact of SeaWinds data on forecasts was investigated. Figure 4(a) shows RMSE of surface wind speed calculated from differences of forecast field and initial field for Test and Control in the Northern Hemisphere (20°N-90°N) for July 2002. SeaWinds data has slightly positive impact after day 6. Positive impact was also recognized in the anomaly correlation of 500 hPa geopotential height particularly in the Northern Hemisphere (Fig.4(b)). Impacts on almost all elements were neutral in December 2001. However, obvious improvement was seen in the Mean Error of 850 hPa geopotential height in the global and tropical (20°N-20°S) regions (Fig.4(c)). Improvement was expected in the Southern Hemisphere because of sparsity of conventional data. However, impacts on 500

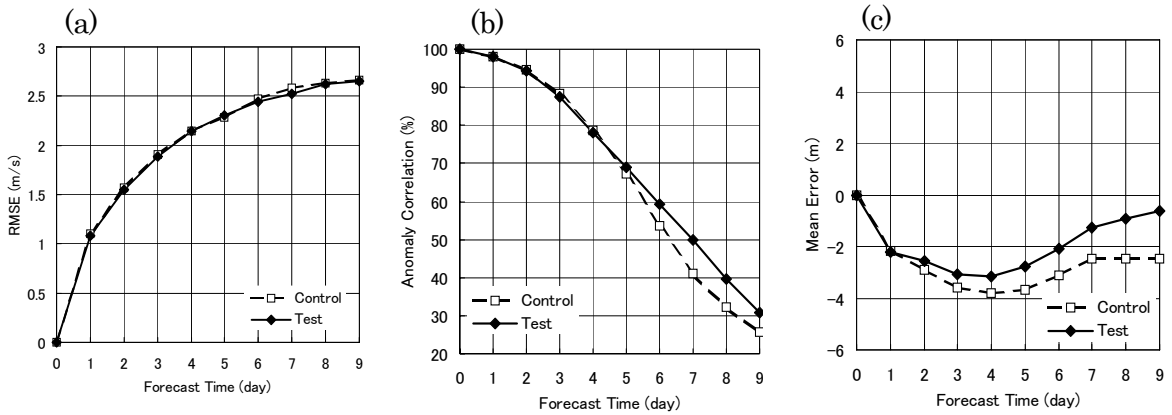


Fig.4 Forecast scores for Test (solid line) and Control (dashed line). (a) RMSE of surface wind speed in the Northern Hemisphere (20°N-90°N) for July 2002. (b) Anomaly correlation of 500 hPa geopotential height in the Northern Hemisphere for July 2002. (c) Mean error of 850 hPa geopotential height in the tropical region (20°N-20°S) for December 2001. The forecasts were started from 12 UTC for the period of 8 to 22 July 2002 (December 2001).

hPa geopotential height and sea level pressure were almost neutral or slightly negative at the end of forecast times.

The experiment was performed to examine the impact on typhoon track forecasts for July 2002. While the impact depends on forecast cases, position errors of typhoon track forecasts decreased in many cases. Figure 5 shows the result of the track forecasts for typhoon T0207 (HALONG) by GSM0103 from the initial time 12 UTC 10 July 2002. The position error of forecasted typhoon track in Test is reduced by as much as 100 km. Figure 6 shows the mean position error of typhoon track forecasts in Test and Control in 36 cases for six typhoons during July 2002. The position error in Test is significantly reduced after 60 hour forecast.

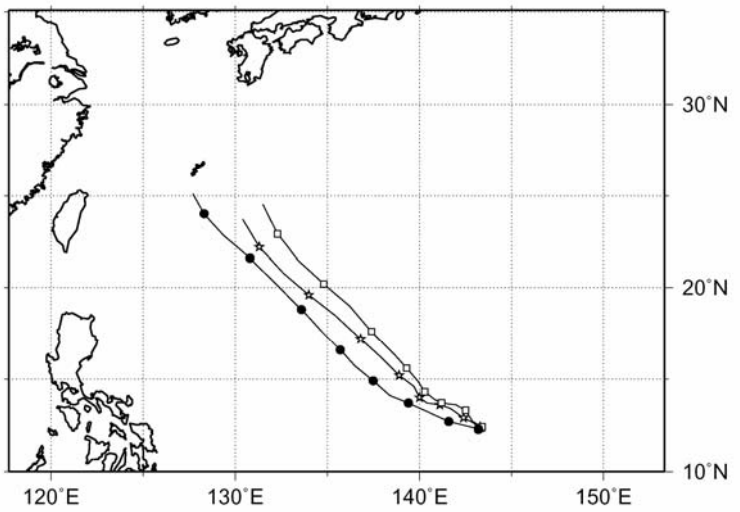


Fig.5 The result of track forecasts for typhoon T0207 (HALONG). Initial time is 12 UTC 10 July 2002. Black circles denote the best track, squares denote Control, and stars denote Test. The symbols are plotted every 12 hours.

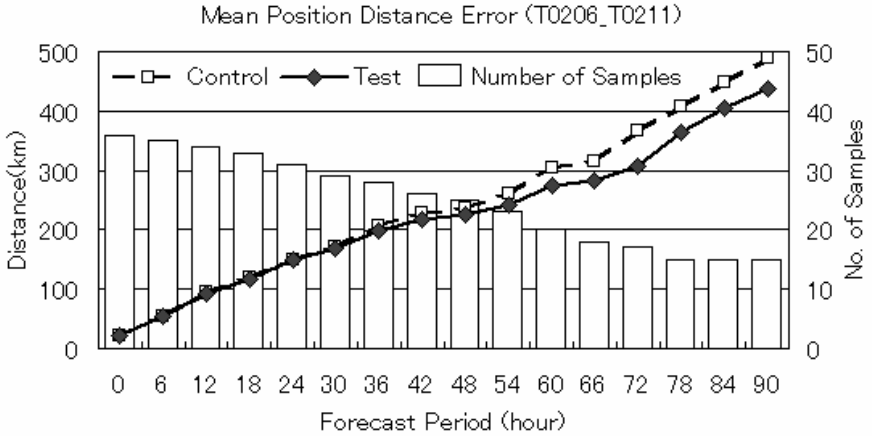


Fig.6 The mean position distance error of forecasted track of typhoons in July 2002. Dashed line denotes Control, solid line denotes Test, and bar denotes the number of samples.

## 4. Conclusions

From the results of the impact study for SeaWinds data, it is evident that forecast scores and typhoon track forecasts are considerably improved by using SeaWinds data. Based on those findings, SeaWinds data have been used in operation since 6 May 2003 at JMA. Further improvement is expected by using data of multiple scatterometers in the future. The ADEOS-II satellite which carried the same type scatterometer SeaWinds as QuikSCAT/SeaWinds was launched by the National Space Development Agency of Japan (NASDA) in December 2002. Unfortunately the spacecraft has not made observations since October 2003 due to its power failure and the data has not been distributed. The Meteorological Operational Polar Satellite (METOP) which carries the Advanced Scatterometer (ASCAT) will be launched by ESA in 2005.

A global 4D-Var data assimilation system is under development as the next operational global data assimilation system at JMA. Using the 4D-Var system, the data in severe weather regions such as fronts or typhoons will be analyzed more correctly because observation time is correctly taken into account.

At the present, the wind vector data contained in Level 2B data are used in the JMA 3D-Var. To use the data more effective for forecasts, assimilation of the original backscattered cross section data or development of a more sophisticated observation operator will be needed.

## References


Ebuchi, N., H. C. Graber and M. J. Caruso, 2002: Evaluation of wind vectors by QuikSCAT /SeaWinds using ocean buoy data. J. Atmos. Oceanic Technol., 19, 2049-2062.

Huddleston, J. N. and B. W. Stiles, 2000: Multi-dimensional Histogram (MUDH) Rain Flag Product Description, Version 3.0, JPL, Pasadena, CA. <http://podaac.jpl.nasa.gov/quikscat/qscat_doc.html>

JMA, 2002: Outline of the operational numerical weather prediction at the Japan Meteorological Agency. Appendix to WMO Numerical Weather Prediction Progress Report, 157pp.

Leidner, S. M., R. N. Hoffman and J. Augenbaum, 2000: SeaWinds Scatterometer Real-Time BUFR Geophysical Data Product. NOAA/ NESDIS.

Tahara, Y, 2000: The preliminary study of the impact of QuikSCAT/SeaWinds ocean surface wind data to the JMA global model. Proc. Fifth International Winds Workshop, Lone, Austria, 169-176.